ORIGINAL RESEARCH

Preoperative Noninvasive Prediction of Recurrence-Free Survival in Hepatocellular Carcinoma Using CT-Based Radiomics Model

Ting Dai [ID], Qian-Biao Gu, Ying-Jie Peng, Chuan-Lin Yu, Peng Liu, Ya-Qiong He [ID]

Department of Radiology, The First Affiliated Hospital of Hunan Normal University (Hunan Provincial People's Hospital), Changsha, Hunan, People's Republic of China

Correspondence: Ya-Qiong He, Email yaqionghe2021@163.com

Purpose: This study aims to explore the value of radiomics combined with clinical parameters in predicting recurrence-free survival (RFS) after the resection of hepatocellular carcinoma (HCC).

Patients and Methods: In this retrospective study, a total of 322 patients with HCC who underwent contrast-enhanced computed tomography (CT) and radical surgical resection were enrolled and randomly divided into a training group (n = 223) and a validation group (n = 97). In the training group, Univariate and multivariate Cox regression analyses were employed to obtain clinical variables related to RFS for constructing the clinical model. The least absolute shrinkage and selection operator (LASSO) and multivariate Cox regression analyses were employed to construct the radiomics model, and the clinical-radiomics model was further constructed. Model prediction performance was subsequently assessed by the area under the time-dependent receiver operating characteristic curve (AUC) and calibration curve. Additionally, Kaplan-Meier analysis was used to evaluate the model's value in predicting RFS. Correlations between radiomics features and pathological parameters were analyzed.

Results: The clinical-radiomics model predicted RFS at 1, 2, and 3 years more accurately than the clinical or radiomics model alone (training group, AUC = 0.834, 0.765 and 0.831, respectively; validation group, AUC = 0.715, 0.710 and 0.793, respectively). The predicted high-risk subgroup based on the clinical-radiomics nomogram had shorter RFS than predicted low-risk subgroup in data sets, enabling risk stratification of various clinical subgroups. Correlation analysis revealed that the rad-score was positively related to microvascular invasion (MVI) and Edmondson-Steiner grade.

Conclusion: The clinical-radiomics model effectively predicts RFS in HCC patients and identifies high-risk individuals for recurrence.

Keywords: Hepatocellular carcinoma, computed tomography, radiomics, recurrence-free survival

Introduction

Hepatocellular carcinoma (HCC) is one of the most prevalent malignant tumors globally, ranking third in causes of cancer-related death, with a 5-year survival rate of about 18%.[1] Currently, radical surgical resection remains the primary treatment strategy for liver cancer, but up to 70% of cases recur within five years, with postoperative tumor recurrence and metastasis being the primary causes of patient mortality.[2] The Barcelona Clinic Liver Cancer (BCLC) staging system is a widely utilized clinical practice guideline,[3] and surgical resection is recommended only for patients with early-stage HCC (BCLC 0, A stage). However, even within the same stage, there are considerable differences in patient prognosis. The treatment and prognosis are often limited by the pre-staging. Studies have shown that liver resection can be extended to advanced HCC (BCLC B, C stage), and that comprehensive treatment of advanced liver cancer can prolong patient survival.[4,5] Furthermore, the clinical outcome of HCC patients is highly correlated with tumor subtype and grade, microvascular invasion, and molecular alterations. While many postoperative prediction models exist, they rely on histopathological information obtained only after biopsy or resection.[6] Thus, non-invasive preoperative prediction of RFS

in HCC patients and identifying high-risk groups for recurrence is vital for guiding clinical decision-making and tailoring treatment strategies.

Radiomics extracts rich quantitative features from medical images at high throughput, transforming them into high-dimensional data for clinical decision support.[7,8] Accumulating research shows that radiomics features are potential prognostic biomarkers for HCC. Combining radiomics with clinical data can improve the prediction of individual recurrence risk post-resection, thereby enhancing clinical benefits.[9–12] Despite its potential, no consensus exists on radiomics prediction models for HCC prognosis, and more evidence is needed. In addition, radiomics can quantify tumor heterogeneity through image texture features, facilitating clinical applications by linking image features to biological bases.[13,14]

This study aims to predict RFS after liver cancer resection based on contrast-enhanced CT radiomics, accurately and non-invasively forecast the HCC prognosis, clarify the prognostic risk, guide clinicians in choosing the most effective treatment plan, and provide more accurate and personalized treatment decisions for liver cancer patients.

Materials and Methods

Patients

This study was approved by the Ethics Committee of Hunan Provincial People's Hospital and fully adhered to the Declaration of Helsinki. All patient information was used anonymously. Given the retrospective nature of the study, the requirement for informed consent was waived. We retrospectively collected 450 patients with pathology diagnosis of single HCC from December 2019 to December 2021 after radical resection at our institution. Inclusion criteria were as follows: (a) age $\geq$ 18 years; (b) contrast-enhanced CT and clinical laboratory examinations performed within two weeks before surgery. Exclusion criteria were as follows: (a) history of other malignancies; (b) extrahepatic metastasis; (c) previous treatments like local ablation and transcatheter arterial chemoembolization; (d) incomplete clinical or imaging data of poor quality. The final research group included 322 patients, randomized into the training group and validation group by a ratio of 7:3 (Figure 1). The workflow chart of necessary steps is presented in Figure 2.

Follow-Up Surveillance

After radical surgical resection, patients were followed up every 3 months during the first year and subsequently every 6 months after that. HCC recurrence was detected by AFP, liver function tests, physical examination, and imaging examinations, which include ultrasound, contrast-enhanced CT, or MRI. The initial event was radical surgical resection. The ending event was recurrence, metastasis, or the last follow-up. Data collection ends on February 29, 2024. The study outcome was RFS, calculated from the initial event to the ending event.

CT Technology

All patients received contrast-enhanced abdomen CT with Siemens Somatom Force or Philips Brilliance iCT 256 CT machine before surgery. The scanning parameters were 2 mm scanning thickness, 5 mm reconstruction thickness, and 120 kV tube voltage with automatic tube current modulation. The arterial, portal venous, and delayed phases were conducted at 25s, 70s, and 150s, respectively, after injection of the contrast agent iohexol 300 (300 mg/mL).

Lesions Segmentation and Conventional CT Evaluation

Using the 3D Slicer (version 5.4.0, https://www.slicer.org/), the volume of interest (VOI) was manually delineated on the portal venous phase images, layer by layer, by a radiologist with 10 years of diagnostic abdominal imaging experience, avoiding blood vessels and bile ducts. Pathology results and clinical data were anonymized during this process. Imaging features evaluated included liver cirrhosis, tumor margin, arterial peritumoral enhancement, tumor pseudocapsule, intratumoral necrosis, hepatic vein invasion, portal vein invasion, and tumor thrombus, reviewed by a professional radiologist with 15 years of experience in diagnostic abdominal imaging.
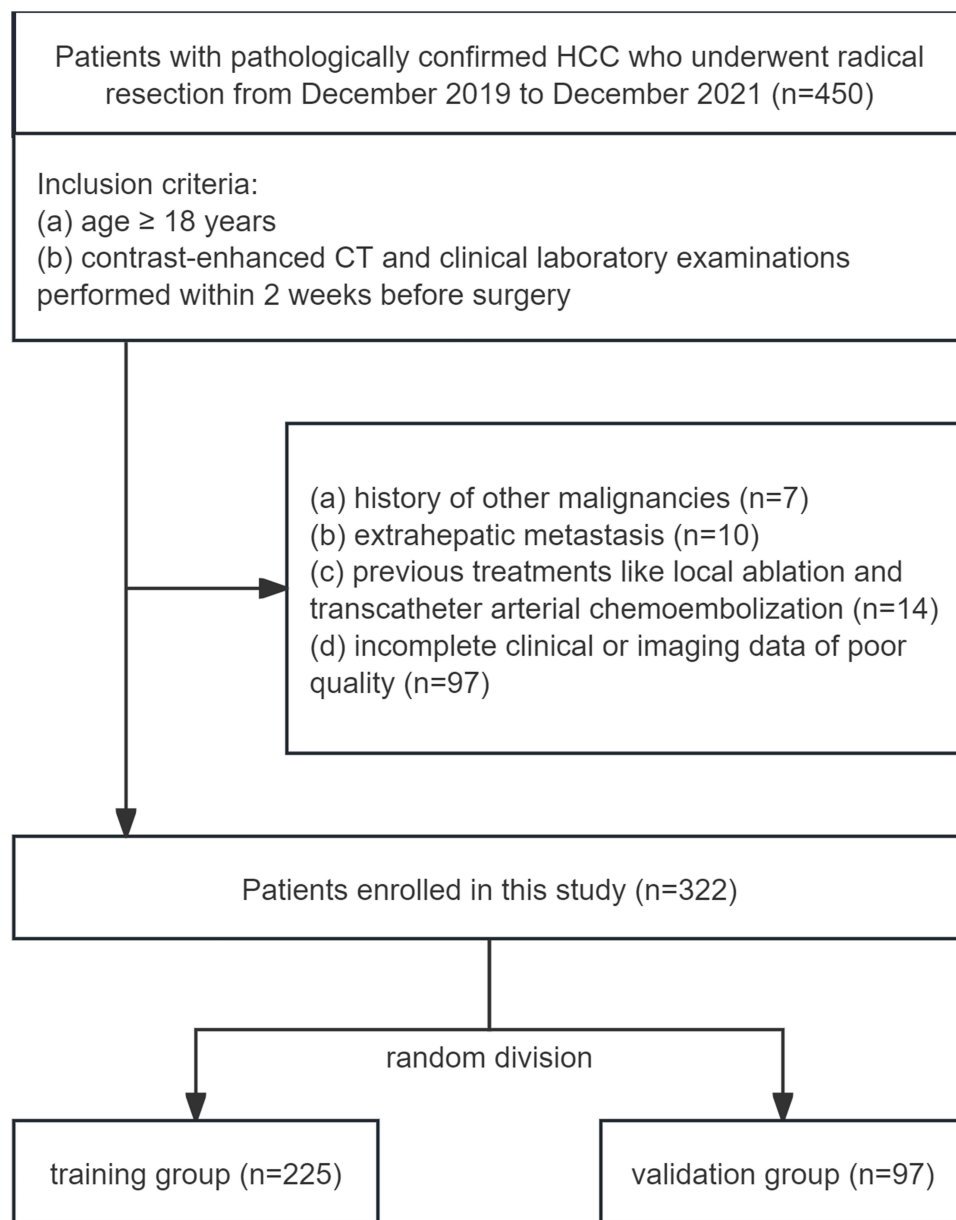
Figure 1 Flowchart shows recruitment pathway for patients.

Radiomics Feature Extraction

The Pyradiomics package (version 2.2.0, https://pyradiomics.readthedocs.io/en/2.2.0/)[15] was used to extract the radiomics features. To reduce image specification differences, the images were resampled at 1×1×1 mm voxels with a bin width of 25. The preprocessed data were then subjected to built-in filtering. Finally, we extracted 1874 radiomics features (14 shape features, 360 first-order features, and 1500 second-order texture features) from each VOI.

Radiomics Signature Construction

Data preprocessing was performed using the Caret package in the R software. First, radiomics features with zero variance and near-zero variance were excluded. Then, predictors with a Spearman correlation coefficient > 0.9 were excluded to select independent predictive features. Data were standardized to reduce the influence of data dimension. LASSO was used to avoid overfitting, and univariate and multivariate Cox regression analyses identified independent radiomics feature predictors associated with postoperative RFS in HCC.
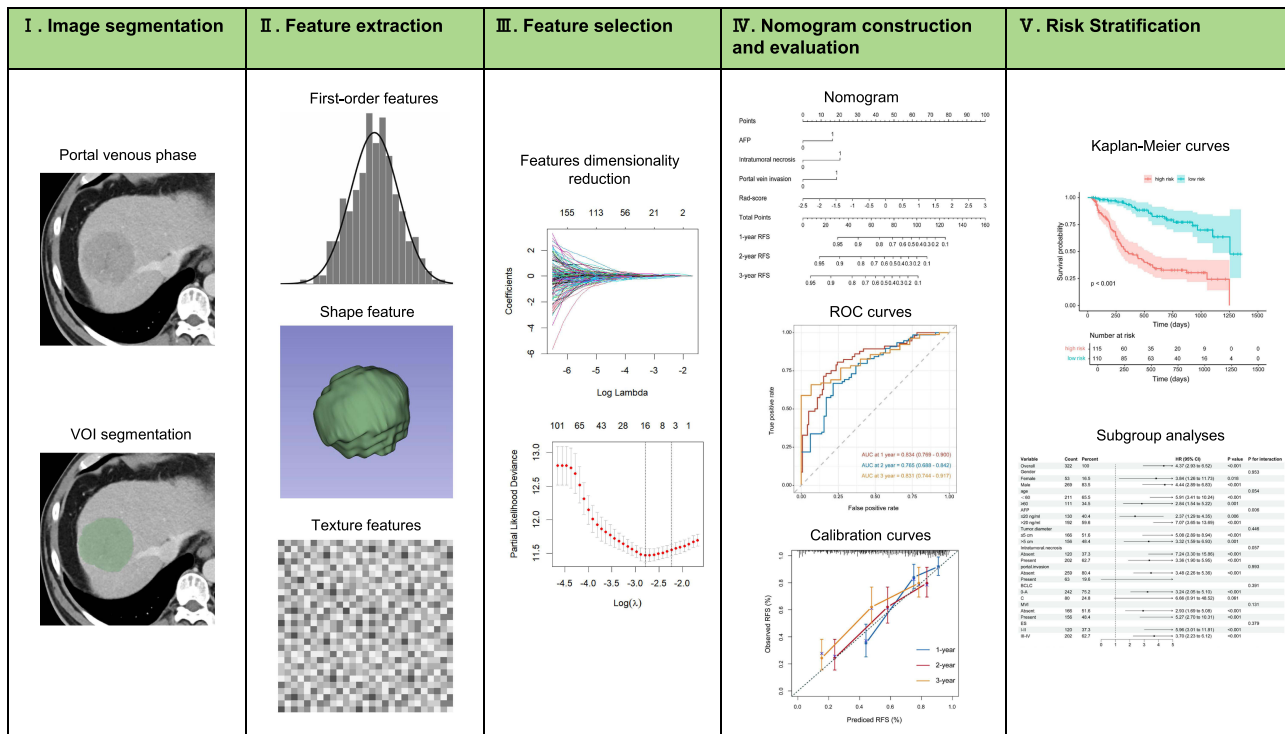
Figure 2 Diagram shows workflow for radiomics image segmentation (I), feature extraction (II), feature selection (III), nomogram construction and evaluation (IV), and risk stratification (V).

Statistical Analysis

Statistical analyses were analyzed using SPSS Statistics software (version 26) and R software (version 4.3.2, http://www.r-project.org). P value < 0.05 was considered statistically significant. According to their distributions, continuous variables and categorical variables were compared using Student's *t*-test or Mann–Whitney *U*-test and χ^2-test, respectively. Model predictive performance was assessed using time-dependent ROC and calibration curves. The optimal cutoff value was identified using the R package "survminer". The survival risk stratification capability was evaluated using Kaplan-Meier analysis along with the Log rank test. Spearman correlation tests explored the relationship between the radiomics score (rad-score) and pathological parameters, thereby investigating the biological background of HCC.

Results

Baseline Characteristics

Table 1 showed the clinical-pathologic characteristics of the patients. Of 322 patients, 130 experienced recurrences. 39.1% of the patients in the training group experienced recurrence with a median RFS of 422 days (interquartile range, 175.5–780 days). 43.3% of the patients in the validation group experienced recurrence with a median RFS of 470 days (interquartile range, 201–808 days). All the included parameters between two datasets showed almost no statistically significant differences.

Radiomic Feature Selection and Signature Construction

Initially, 1874 features were extracted from the VOI of each patient. After preprocessing, 1555 irrelevant features were removed, and 319 features remained that contributed to predicting RFS. Sixteen features were identified after the LASSO

Table 1 Baseline Characteristics of the Training and Validation Group

Characteristic		Total (n = 322)	Training Group (n = 225)	Validation Group (n = 97)	P value
Recurrence status	No	192 (59.63)	137 (60.89)	55 (56.70)	0.482
	Yes	130 (40.37)	88 (39.11)	42 (43.30)	
RFS, Median (P25, P75), days		439.5 (182, 782)	422 (175.5, 780)	470 (201, 808)	0.437
Age, mean ± SD, years		54.57 ± 11.28	54.90 ± 11.50	53.79 ± 10.78	0.421
Gender	Female	53 (16.46)	36 (16.00)	17 (17.53)	0.735
	Male	269 (83.54)	189 (84.00)	80 (82.47)	
AFP	≤20 ng/mL	130 (40.37)	90 (40.00)	40 (41.24)	0.836
	>20 ng/mL	192 (59.63)	135 (60.00)	57 (58.76)	
CEA	≤5 ng/mL	301 (93.48)	212 (94.22)	89 (91.75)	0.410
	>5 ng/mL	21 (6.52)	13 (5.78)	8 (8.25)	
CA199	≤37 U/mL	276 (85.71)	192 (85.33)	84 (86.60)	0.766
	>37 U/mL	46 (14.29)	33 (14.67)	13 (13.40)	
HBV-DNA	≤100 IU/mL, %	130 (40.37)	92 (40.89)	38 (39.18)	0.774
	> 100 IU/mL, %	192 (59.63)	133 (59.11)	59 (60.82)	
HBsAg	<0.05 IU/ML	58 (18.01)	36 (16.00)	22 (22.68)	0.152
	≥0.05 IU/ML	264 (81.99)	189 (84.00)	75 (77.32)	
ALB	<35 g/L	297 (92.24)	207 (92.00)	90 (92.78)	0.810
	≥35 g/L	25 (7.76)	18 (8.00)	7 (7.22)	
TBIL	≤20.4 umol/L	266 (82.61)	181 (80.44)	85 (87.63)	0.119
	>20.4 umol/L	56 (17.39)	44 (19.56)	12 (12.37)	
ALT	≤50 U/L	244 (75.78)	166 (73.78)	78 (80.41)	0.202
	>50 U/L	78 (24.22)	59 (26.22)	19 (19.59)	
AST	≤40 U/L	202 (62.73)	142 (63.11)	60 (61.86)	0.831
	>40 U/L	120 (37.27)	83 (36.89)	37 (38.14)	
PT	≤12.5 S	300 (93.17)	209 (92.89)	91 (93.81)	0.763
	>12.5 S	22 (6.83)	16 (7.11)	6 (6.19)	
Fibrinogen	≤4 g/L	267 (82.92)	189 (84.00)	78 (80.41)	0.433
	>4 g/L	55 (17.08)	36 (16.00)	19 (19.59)	
Tumor diameter	≤5 cm	166 (51.55)	119 (52.89)	47 (48.45)	0.465
	>5 cm	156 (48.45)	106 (47.11)	50 (51.55)	
Liver cirrhosis	Absent	214 (66.46)	145 (64.44)	69 (71.13)	0.243
	Present	108 (33.54)	80 (35.56)	28 (28.87)	
Tumor margin	Smooth	196 (60.87)	135 (60.00)	61 (62.89)	0.626
	Nonsmooth	126 (39.13)	90 (40.00)	36 (37.11)	
Arterial peritumoral enhancement	Absent	273 (84.78)	191 (84.89)	82 (84.54)	0.936
	Present	49 (15.22)	34 (15.11)	15 (15.46)	
Tumor pseudocapsule	Absent	207 (64.29)	145 (64.44)	62 (63.92)	0.928
	Present	115 (35.71)	80 (35.56)	35 (36.08)	
Intratumoral necrosis	Absent	120 (37.27)	84 (37.33)	36 (37.11)	0.970
	Present	202 (62.73)	141 (62.67)	61 (62.89)	
Hepatic vein invasion	Negative	273 (84.78)	189 (84.00)	84 (86.60)	0.552
	Positive	49 (15.22)	36 (16.00)	13 (13.40)	
Portal vein invasion	Negative	259 (80.43)	179 (79.56)	80 (82.47)	0.545
	Positive	63 (19.57)	46 (20.44)	17 (17.53)	
Portal vein tumor thrombus	Negative	306 (95.03)	212 (94.22)	94 (96.91)	0.461
	Positive	16 (4.97)	13 (5.78)	3 (3.09)	
BCLC	0-A	242 (75.16)	168 (74.67)	74 (76.29)	0.757
	C	80 (24.84)	57 (25.33)	23 (23.71)	
Edmondson-Steiner grade	I–II	120 (37.27)	83 (36.89)	37 (38.14)	0.831
	III–IV	202 (62.73)	142 (63.11)	60 (61.86)	

(Continued)

Table 1 (Continued).

Characteristic		Total (n = 322)	Training Group (n = 225)	Validation Group (n = 97)	P value
MVI	Absent	166 (51.55)	123 (54.67)	43 (44.33)	0.089
	Present	156 (48.45)	102 (45.33)	54 (55.67)	
KI67	≤10%	97 (30.12)	58 (25.78)	39 (40.21)	0.010
	>10%	225 (69.88)	167 (74.22)	58 (59.79)	
CK19	Absent	225 (69.88)	151 (67.11)	74 (76.29)	0.100
	Present	97 (30.12)	74 (32.89)	23 (23.71)	

Abbreviations: RFS, recurrence-free survival; SD, standard deviation; AFP, alpha-fetoprotein; CEA, carcinoembryonic antigen; CA199, carbohydrate antigen 19–9; HBV-DNA, hepatitis B virus deoxyribonucleic acid; HBsAg, hepatitis B surface antigen; ALB, albumin; TBIL, total bilirubin; ALT, alanine aminotransferase; AST, aspartate aminotransferase; PT, prothrombin time; BCLC, stage of Barcelona clinic liver cancer; MVI, microvascular invasion; CK19, cytokeratin 19.

algorithm, and six feature variables were obtained through univariate and multivariate Cox regression analyses, which were utilized to construct the radiomics model and calculate the rad-score (Table S1). The calculation formula was:

$$
\begin{aligned}
\mathrm{rad-score} = {} & 0.24 \times \mathrm{auto\_gradient\_first\,order\_Kurtosis} \\
& + 0.2 \times \mathrm{auto\_log-sigma-3-0-mm-3D\_glszm\_Large\,Area\,Low\,Gray\,Level\,Emphasis} \\
& - (0.32 \times \mathrm{auto\_original\_glszm\_Small\,Area\,Low\,Gray\,Level\,Emphasis}) \\
& - (0.3 \times \mathrm{auto\_original\_shape\_Sphericity}) \\
& - (0.39 \times \mathrm{auto\_wavelet-HHL\_gldm\_Dependence\,Variance})
\end{aligned}
$$

Model Development and Validation

In the training group, univariate analysis identified AFP, HBV-DNA, fibrinogen, ALT, AST, tumor diameter, liver cirrhosis, tumor margin, arterial peritumoral enhancement, tumor pseudocapsule, intratumoral necrosis, venous invasion, portal invasion, portal vein tumor thrombus as potential risk variables for RFS (p < 0.05). Multivariate analysis indicated AFP (HR = 1.95; 95% CI: 1.20–3.18; P = 0.007), intratumoral necrosis (HR = 2.91; 95% CI: 1.55–5.44; P < 0.001), and portal invasion (HR = 2.28; 95% CI: 1.27–4.10; P = 0.006) were independently linked with HCC prognosis (Table 2). These factors, along with and without the rad-score, were included in the clinical model and the clinical-radiomics model, which were finally displayed through nomograms (Figure 3A). Compared to the clinical and radiomics models, the clinical-radiomics model demonstrated superior predictive performance, with an AUC for 1, 2, and 3 years RFS of 0.834(0.769–0.900), 0.765(0.688–0.842), 0.831(0.744–0.917) in the training group, respectively, and 0.715(0.591–0.839), 0.710(0.590–0.830), 0.793(0.669–0.918) in the validation group, respectively (Figure 3B and C). The calibration curves indicated well calibrated between model-predicted and observed probability of RFS (Figure 3D and E).

Survival Risk Stratification

Based on the optimal cutoff value of the clinical-radiomics score, the cohort was divided into low-risk (clinical-radiomics score < 1.38) and high-risk (clinical-radiomics score ≥ 1.38) subgroups. As illustrated by the Kaplan-Meier curves in Figure 4, the low-risk subgroup exhibited longer RFS than the high-risk subgroup, with patients having higher scores facing a greater risk of recurrence (HR = 3.13; 95% CI: 1.70–5.79; P < 0.001). Subgroup analyses revealed that the model applied to different populations and stratified patient prognostic risk (Figure 5).

Correlation with Pathologic Parameters

We further explored the correlation between radiomics features and pathological parameters. The results demonstrated that the rad-score was positively linked to known pathological parameters associated with HCC prognosis, including tumor MVI (P<0.001) and Edmondson-Steiner grade (P<0.05) (Figure 6).

Table 2 Univariate and Multivariable Cox Regression Analysis of Predictors of Recurrence-Free Survival

| Variables	Univariable Analysis		Multivariable Analysis	
	HR (95% CI)	P value	HR (95% CI)	P value
Age	0.99 (0.97–1.01)	0.347		
Sex, Male vs Female	1.19 (0.66–2.15)	0.566		
AFP, > 20 ng/mL vs ≤20 ng/mL	2.09 (1.32 ~ 3.31)	0.002*	1.95 (1.20–3.18)	0.007*
CEA, > 5 ng/mL vs ≤ 5 ng/mL	0.73 (0.26–1.99)	0.533		
CA199, > 37 U/ mL vs ≤ 37 U/ mL	1.05 (0.58–1.90)	0.871		
HBV-DNA, > 100 IU/mL, % vs ≤ 100 IU/mL, %	2.57 (1.56 ~ 4.23)	<0.001*	1.47 (0.85–2.55)	0.167
HBSAG, ≥0.05 IU/ML vs < 0.05 IU/ML	1.23 (0.65 ~ 2.32)	0.517		
ALB, ≥35 g/L vs <35 g/L	1.68 (0.81–3.48)	0.166		
TBIL, > 20.4 umol/L vs ≤20.4 umol/L	1.31 (0.80–2.14)	0.288		
ALT, >50 U/L vs ≤50 U/L	1.64 (1.05–2.56)	0.029*	1.03 (0.59–1.82)	0.912
AST, >40 U/L vs ≤40 U/L	2.46 (1.61–3.76)	<0.001*	1.77 (0.99–3.14)	0.053
PT, >12.5 S vs ≤12.5 S	0.95 (0.41–2.17)	0.895		
Fibrinogen, > 4 g/dL vs ≤ 4 g/dL	1.71 (1.03–2.85)	0.039*	0.68 (0.38–1.23)	0.202
Tumor diameter, >5 cm vs ≤5 cm	2.49 (1.60–3.85)	<0.001*	1.01 (0.58–1.78)	0.963
Liver cirrhosis, Present vs Absent	0.93 (0.60–1.44)	0.753		
Tumor margin, Nonsmooth vs Smooth	1.76 (1.15–2.68)	0.009*	0.99 (0.61–1.59)	0.956
Arterial peritumoral enhancement, Present vs Absent	1.74 (1.02–2.98)	0.043*	1.78 (0.99–3.21)	0.054
Tumor pseudocapsule, Present vs Absent	0.56 (0.35–0.91)	0.019*	0.60 (0.36–1.00)	0.051
Intratumoral necrosis, Present vs Absent	3.47 (2.03–5.93)	<0.001*	2.91 (1.55–5.44)	0.001*
Hepatic vein invasion, Positive vs Negative	2.69 (1.64–4.39)	<0.001*	0.80 (0.44–1.45)	0.460
Portal vein invasion, Positive vs Negative	3.67 (2.33–5.79)	<0.001*	2.28 (1.27–4.10)	0.006*
Portal vein tumor thrombus, Positive vs Negative	2.97 (1.43–6.17)	0.004*	1.22 (0.52–2.86)	0.653

Note: *P value indicates statistically significant.
Abbreviations: HR, hazard ratio; CI, confidence interval.

Discussion

In this study, we developed and validated a model for predicting RFS after HCC resection based on contrast-enhanced CT radiomics. The model's effectiveness in risk stratification across different subgroups and its correlation with pathological parameters were evaluated. The clinical-radiomics model showed a better ability to predict RFS than the clinical or radiomics models alone and was applicable across various clinical subgroups. Additionally, we found that the rad-score was positively linked to tumor microvascular invasion and Edmondson-Steiner grade.

The recurrence rate of HCC after radical resection is high,[2] and it is essential to accurately predict the RFS and identify the high-risk recurrence individuals for clinical treatment decision-making. Currently, numerous radiomics-based models have been constructed to predict HCC patients' recurrence risk and prognosis.[10,16–19] However, these studies had imperfections such as limited inclusion of clinical or imaging indicators, relatively small sample sizes, acquisition of radiomics features in two-dimensional regions of interest, and inclusion of postoperative pathological parameters in the models. Our study incorporated more comprehensive preoperative clinical indicators and subjective imaging features with radiomics, aiming to assess the worth of integrating radiomics with clinical parameters in predicting postoperative RFS in HCC patients. Additionally, we attempted to explore the correlation between radiomics features and pathological parameters. We found that AFP, intratumoral necrosis, and portal invasion were recognized as independent prognostic variables for RFS in HCC patients in the present study. AFP is a serum marker highly relevant to the screening, diagnosis, and surveillance of HCC. High serum AFP levels are a risk variable for tumor recurrence and poor prognosis, consistent with our findings.[20] In exploratory analyses, we noted that in the AFP subgroup, the P for interaction was < 0.05 and the hazard ratio was higher in the AFP-positive population (HR = 7.07, 95% CI: 3.65–13.69), suggesting that the model predicts more effectively in this population. Another significant predictor in our analysis was the occurrence of necrosis within the tumor. Studies have shown that rapid tumor growth leads to tissue hypoxia and necrosis in the tumor's central area, and tumor necrosis debris induces inflammation and immunomodulation, which promotes changes in the
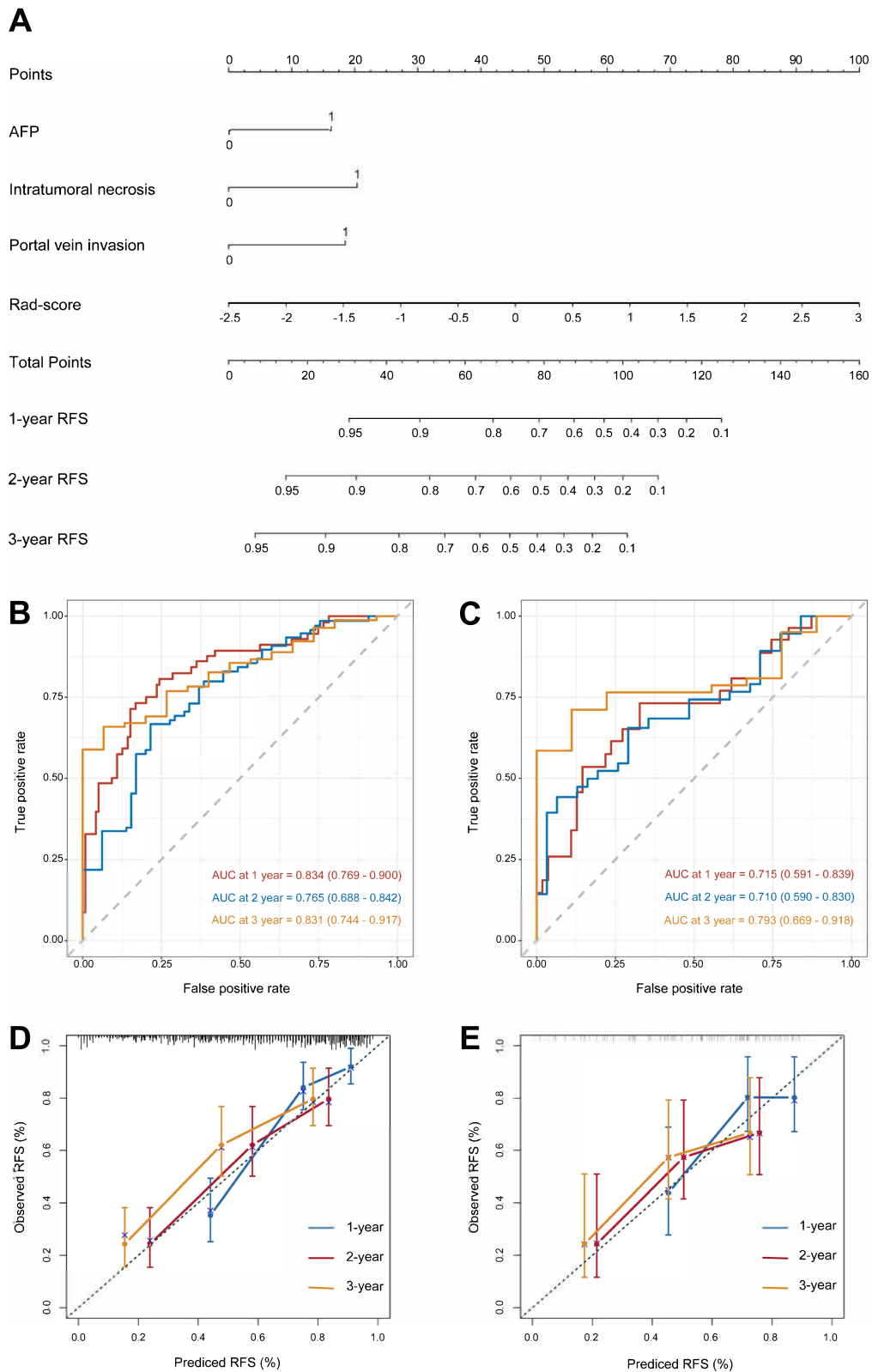
Figure 3 Nomogram, time-dependent ROC curves and calibration curves. Clinical-radiomics nomogram (**A**). Time-dependent receiver operating characteristic curves for predicting 1-year, 2-year, and 3-year RFS in the training group (**B**) and validation group (**C**). The calibration curves of clinical-radiomics nomogram in the training group (**D**) and validation group (**E**).
**Abbreviations**: Rad-score, radiomics score; AUC, area under the curve.
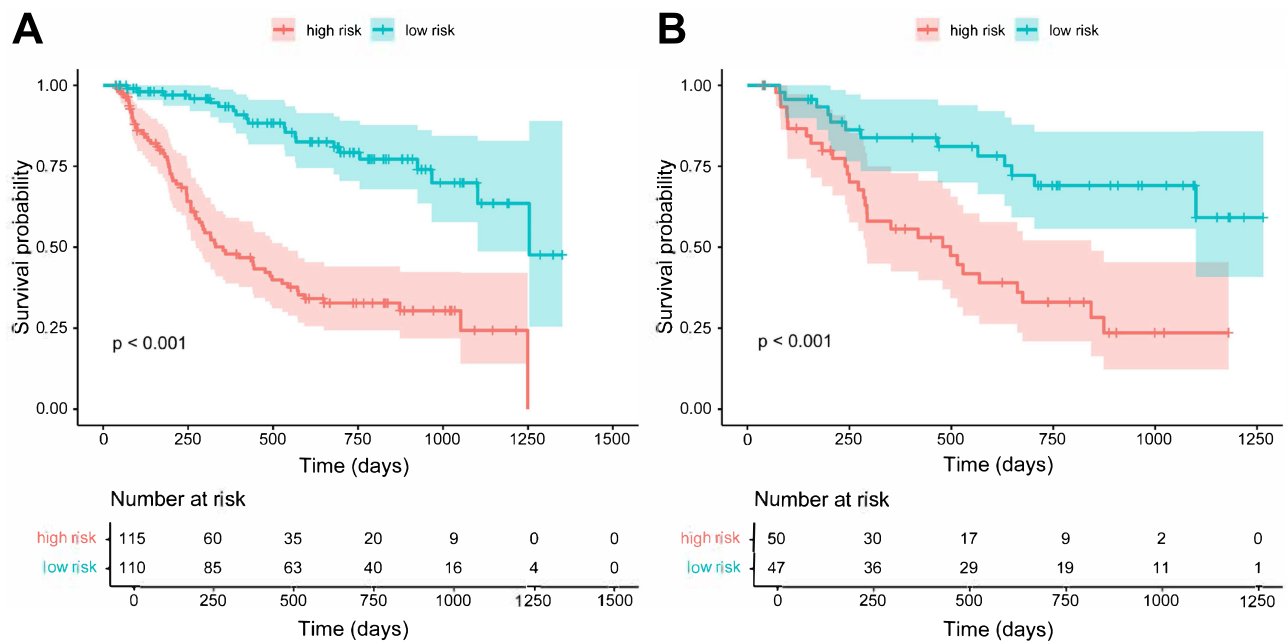
Figure 4 Risk stratification of clinical-radiomics nomogram. Kaplan-Meier curves and Log rank test for the training group (**A**) and validation group (**B**).

Variable	Count	Percent		HR (95% CI)	P value	P for interaction
Overall	322	100		4.37 (2.93 to 6.52)	<0.001	
Gender						0.953
Female	53	16.5		3.84 (1.26 to 11.73)	0.018	
Male	269	83.5		4.44 (2.89 to 6.83)	<0.001	
Age						0.054
<60 years old	211	65.5		5.91 (3.41 to 10.24)	<0.001	
≥60 years old	111	34.5		2.84 (1.54 to 5.22)	0.001	
AFP						0.006
≤20 ng/ml	130	40.4		2.37 (1.29 to 4.35)	0.006	
≥20 ng/ml	192	59.6		7.07 (3.65 to 13.69)	<0.001	
Tumor.diameter						0.446
≤5 cm	166	51.6		5.08 (2.89 to 8.94)	<0.001	
>5 cm	156	48.4		3.32 (1.59 to 6.93)	0.001	
BCLC						0.391
0-A	242	75.2		3.24 (2.05 to 5.10)	<0.001	
C	80	24.8		6.66 (0.91 to 48.52)	0.061	
MVI						0.131
Absent	166	51.6		2.93 (1.69 to 5.08)	<0.001	
Present	156	48.4		5.27 (2.70 to 10.31)	<0.001	
ES						0.379
I-II	120	37.3		5.96 (3.01 to 11.81)	<0.001	
III-IV	202	62.7		3.70 (2.23 to 6.12)	<0.001	

Figure 5 Subgroup analysis for the risk stratification of clinical-radiomics nomogram.
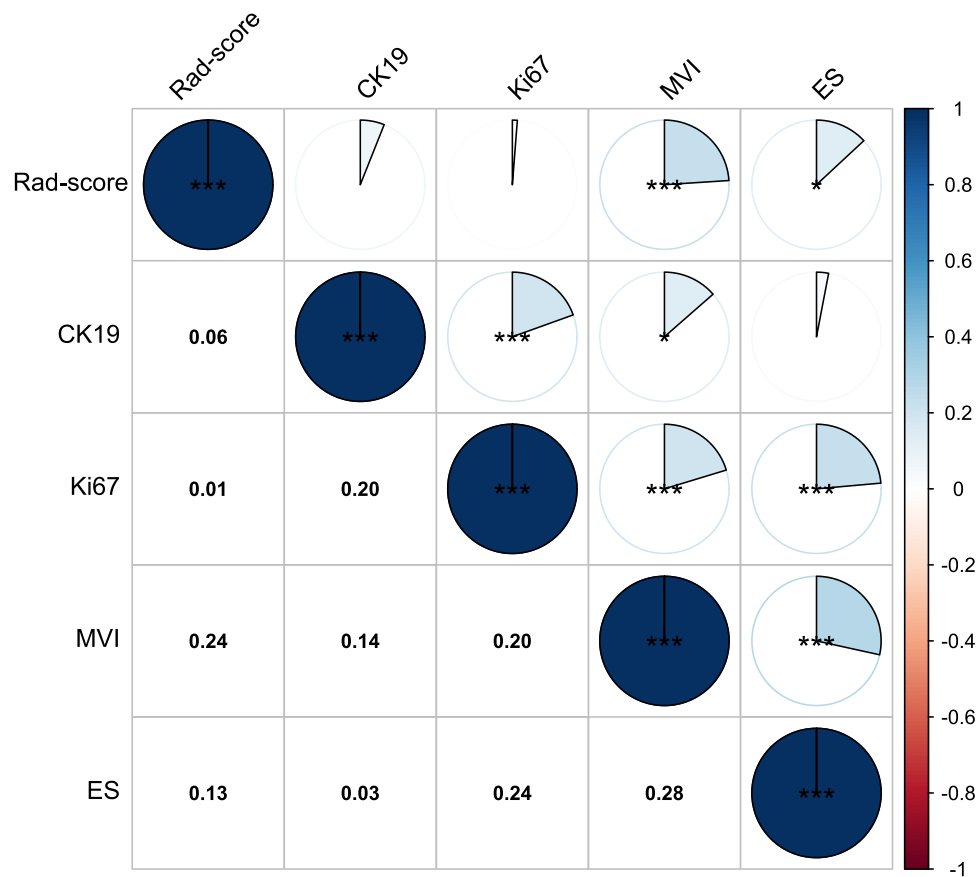
Figure 6 The association between radiomics features and pathological parameters.
Notes: *P value indicates less than 0.05, ***P value indicates less than 0.001.

tumor microenvironment and leads to immune escape.[21–23] This has adverse effects on the clinical outcomes of patients with liver cancer, pancreatic cancer, gallbladder cancer, and colorectal cancer,[24–28] which is similar to our findings. Macrovascular invasion reflects the aggressive biological behavior of tumors and is correlated with worse clinical outcomes.[29] In agreement with previous studies, portal vein invasion is another risk variable for poor clinical outcome. HCC patients with vascular infiltration face a higher risk of recurrence and shorter survival following resection.[30–32] Additionally, some clinical variables, including liver cirrhosis, tumor size, and arterial peritumoral enhancement, have been regarded as independent factors predicting the prognosis of HCC.[16,17,33] In this study, univariate analysis indicated that these characteristics were significantly related to RFS, but they did not retain statistical significance in multivariate analysis, possibly due to selection bias or interactions among variables. It is well known that MVI and Edmondson-Steiner grade is one of the clinicopathological factors associated with HCC prognosis, and its appearance represents more aggressive tumor biological behavior, which is related to higher recurrence rates and lower survival rates.[34,35] The study results indicated that rad-score was associated with known pathological prognostic outcomes, suggesting that radiomics features might reflect underlying tumor biological behaviors. In the future, more convincing evidence needs to be explored to promote the exploration of tumor microstructure complexity and biological context.

Our study had limitations. First, this was a retrospective study. Second, this study did not perform external validation. Therefore, prospective, multicenter studies were needed to obtain more credible clinical application evidence. Third, we only delineated the tumor region's volume, which may have overlooked information from the surrounding tumor area. Finally, manual segmentation of VOI was time-consuming and labor-intensive, requiring fully automatic or semi-automatic delineation to simplify the process and improve work efficiency.

Conclusion

In summary, the clinical-radiomics model, which is based on contrast-enhanced CT radiomics and clinical parameters, can non-invasively assess postoperative RFS in HCC patients and identify high-risk individuals for recurrence, which has good clinical utility for predicting the postoperative outcome and guiding personalized treatment decisions.

Abbreviations

HCC, hepatocellular carcinoma; CT, computed tomography; RFS, recurrence-free survival; LASSO, least absolute shrinkage and selection operator; AUC, area under the curve; Rad-score, radiomics score; CEA, carcinoembryonic antigen; AFP, alpha-fetoprotein; CA199, carbohydrate antigen 19-9; HBsAg, hepatitis B surface antigen; HBV-DNA, hepatitis B virus deoxyribonucleic acid; TBIL, total bilirubin; ALT, alanine aminotransferase; AST, aspartate aminotransferase; ALB, albumin; PT, prothrombin time; MVI, microvascular invasion; BCLC, Barcelona Clinic Liver Cancer; ES, Edmondson-Steiner grade; CK19, cytokeratin 19; VOI, volume of interest; ROC, receiver operating characteristic; SD, standard deviation; HR, hazard ratio; CI, confidence interval.

Ethics Approval and Informed Consent

The retrospective study, approved by the ethics committee of The First Affiliated Hospital of Hunan Normal University (Hunan Provincial People's Hospital) and fully adhered to the Declaration of Helsinki, waived the requirement of written informed consent.

Author Contributions

All authors made a significant contribution to the work reported, whether that is in the conception, study design, execution, acquisition of data, analysis and interpretation, or in all these areas; took part in drafting, revising or critically reviewing the article; gave final approval of the version to be published; have agreed on the journal to which the article has been submitted; and agree to be accountable for all aspects of the work.

Funding

Disclosure

The authors have no conflicts of interest in this work.

References

1. Vogel A, Meyer T, Sapisochin G, Salem R, Saborowski A. Hepatocellular carcinoma. *Lancet*. 2022;400(10360):1345–1362. doi:10.1016/S0140-6736(22)01200-4
2. Galle PR, Forner A, Llovet JM, et al. EASL clinical practice guidelines: management of hepatocellular carcinoma. *J Hepatol*. 2018;69(1):182–236. doi:10.1016/j.jhep.2018.03.019
3. Reig M, Forner A, Rimola J, et al. BCLC strategy for prognosis prediction and treatment recommendation: the 2022 update. *J Hepatol*. 2022;76 (3):681–693. doi:10.1016/j.jhep.2021.11.018
4. Qi X, Wang D, Su C, Li H, Guo X. Hepatic resection versus transarterial chemoembolization for the initial treatment of hepatocellular carcinoma: a systematic review and meta-analysis. *Oncotarget*. 2015;6(21):18715–18733. doi:10.18632/oncotarget.4134
5. Yang B, Zheng B, Yang M, et al. Liver resection versus transarterial chemoembolization for the initial treatment of Barcelona clinic liver cancer stage B hepatocellular carcinoma. *Hepatol Int*. 2018;12(5):417–428. doi:10.1007/s12072-018-9888-4
6. Ronot M, Chernyak V, Burgoyne A, et al. Imaging to predict prognosis in hepatocellular carcinoma: current and future perspectives. *Radiology*. 2023;307(3). doi:10.1148/radiol.221429
7. Lambin P, Leijenaar RTH, Deist TM, et al. Radiomics: the bridge between medical imaging and personalized medicine. *Nat Rev Clin Oncol*. 2017;14(12):749–762. doi:10.1038/nrclinonc.2017.141
8. Bi WL, Hosny A, Schabath MB, et al. Artificial intelligence in cancer imaging: clinical challenges and applications. *Ca a Cancer J Clinicians*. 2019;69(2):127–157. doi:10.3322/caac.21552
9. Ji G-W, Zhu F-P, Xu Q, et al. Machine-learning analysis of contrast-enhanced CT radiomics predicts recurrence of hepatocellular carcinoma after resection: a multi-institutional study. *EBioMedicine*. 2019;50:156–165. doi:10.1016/j.ebiom.2019.10.057
10. Li Z, Yu J, Li Y, et al. Preoperative radiomics nomogram based on CT image predicts recurrence-free survival after surgical resection of hepatocellular carcinoma. *Acad Radiol*. 2023;30(8):1531–1543. doi:10.1016/j.acra.2022.12.039

11. Jin J, Jiang Y, Zhao Y-L, Huang P-T. Radiomics-based machine learning to predict the recurrence of hepatocellular carcinoma: a systematic review and meta-analysis. *Acad Radiol*. 2024;31(2):467–479. doi:10.1016/j.acra.2023.09.008

12. Chong -H-H, Yang L, Sheng R-F, et al. Multi-scale and multi-parametric radiomics of gadoxetate disodium–enhanced MRI predicts microvascular invasion and outcome in patients with solitary hepatocellular carcinoma ≤ 5 cm. *Eur Radiol*. 2021;31(7):4824–4838. doi:10.1007/s00330-020-07601-2

13. Tomaszewski MR, Gillies RJ. The biological meaning of radiomic features. *Radiology*. 2021;298(3):505–516. doi:10.1148/radiol.2021202553

14. Bera K, Braman N, Gupta A, Velcheti V, Madabhushi A. Predicting cancer outcomes with radiomics and artificial intelligence in radiology. *Nat Rev Clin Oncol*. 2021;19(2):132–146. doi:10.1038/s41571-021-00560-7

15. van Griethuysen JJM, Fedorov A, Parmar C, et al. Computational radiomics system to decode the radiographic phenotype. *Cancer Res*. 2017;77 (21):e104–e107. doi:10.1158/0008-5472.CAN-17-0339

16. Wang F, Chen Q, Zhang Y, et al. CT-based radiomics for the recurrence prediction of hepatocellular carcinoma after surgical resection. *J Hepatocell Carcinoma*. 2022;9:453–465. doi:10.2147/JHC.S362772

17. Liu Q, Li J, Liu F, et al. A radiomics nomogram for the prediction of overall survival in patients with hepatocellular carcinoma after hepatectomy. *Cancer Imaging*. 2020;20(1). doi:10.1186/s40644-020-00360-9

18. Deng P-Z, Zhao B-G, Huang X-H, et al. Preoperative contrast-enhanced computed tomography-based radiomics model for overall survival prediction in hepatocellular carcinoma. *World J Gastroenterol*. 2022;28(31):4376–4389. doi:10.3748/wjg.v28.i31.4376

19. Li N, Wan X, Zhang H, Zhang Z, Guo Y, Hong D. Tumor and peritumor radiomics analysis based on contrast-enhanced CT for predicting early and late recurrence of hepatocellular carcinoma after liver resection. *BMC Cancer*. 2022;22(1):1. doi:10.1186/s12885-022-09743-6.

20. Hu X, Chen R, Wei Q, Xu X. The landscape of alpha fetoprotein in hepatocellular carcinoma: where are we? *Int J Bio Sci*. 2022;18(2):536–551. doi:10.7150/ijbs.64537

21. Chen Q, Wang J, Zhang Q, et al. Tumour cell-derived debris and IgG synergistically promote metastasis of pancreatic cancer by inducing inflammation via tumour-associated macrophages. *Br. J. Cancer*. 2019;121(9):786–795. doi:10.1038/s41416-019-0595-2

22. Zhang J, Zhang Q, Lou Y, et al. Hypoxia-inducible factor-1α/interleukin-1β signaling enhances hepatoma epithelial–mesenchymal transition through macrophages in a hypoxic-inflammatory microenvironment. *Hepatology*. 2018;67(5):1872–1889. doi:10.1002/hep.29681

23. Crusz SM, Balkwill FR. Inflammation and cancer: advances and new agents. *Nat Rev Clin Oncol*. 2015;12(10):584–596. doi:10.1038/nrclinonc.2015.105

24. Wei T, Zhang X-F, Bagante F, et al. Tumor necrosis impacts prognosis of patients undergoing curative-intent hepatocellular carcinoma. *Ann Surg Oncol*. 2020;28(2):797–805. doi:10.1245/s10434-020-09390-w

25. Yang S, Hu H, Hu Y, et al. Is tumor necrosis a clinical prognostic factor in hepato-biliary-pancreatic cancers? A systematic review and meta-analysis. *Cancer Med*. 2023;12(10):11166–11176. doi:10.1002/cam4.5742

26. Xie T, Xie X, Liu W, Chen L, Liu K, Zhou Z. Prediction of postoperative recurrence in resectable pancreatic body/tail adenocarcinoma: a novel risk stratification approach using a CT-based nomogram. *Eur Radiol*. 2023;33(11):7782–7793. doi:10.1007/s00330-023-10047-x

27. Yang S-Q, Wang J-K, Ma W-J, et al. Prognostic significance of tumor necrosis in patients with gallbladder carcinoma undergoing curative-intent resection. *Ann Surg Oncol*. 2023;31(1):125–132. doi:10.1245/s10434-023-14421-3

28. Richards CH, Roxburgh CSD, Anderson JH, et al. Prognostic value of tumour necrosis and host inflammatory responses in colorectal cancer. *Br J Surg*. 2012;99(2):287–294. doi:10.1002/bjs.7755

29. Roayaie S, Blume IN, Thung SN, et al. A system of classifying microvascular invasion to predict outcome after resection in patients with hepatocellular carcinoma. *Gastroenterology*. 2009;137(3):850–855. doi:10.1053/j.gastro.2009.06.003

30. Liu L, Qin S, Lin K, et al. Development and comprehensive validation of a predictive prognosis model for very early HCC recurrence within one year after curative resection: a multicenter cohort study. *Int j Surg*. 2024;110(6):3401–11. doi:10.1097/JS9.0000000000001467.

31. Shah SA, Cleary SP, Wei AC, et al. Recurrence after liver resection for hepatocellular carcinoma: risk factors, treatment, and outcomes. *Surgery*. 2007;141(3):330–339. doi:10.1016/j.surg.2006.06.028

32. Zhang Z, Jiang H, Chen J, et al. Hepatocellular carcinoma: radiomics nomogram on gadoxetic acid-enhanced MR imaging for early postoperative recurrence prediction. *Cancer Imaging*. 2019;19(1). doi:10.1186/s40644-019-0209-5

33. Cao X, Yang H, Luo X, et al. A cox nomogram for assessing recurrence free survival in hepatocellular carcinoma following surgical resection using dynamic contrast-enhanced MRI radiomics. *J Magn Reson Imaging*. 2023;58(6):1930–1941. doi:10.1002/jmri.28725

34. Lei Z, Li J, Wu D, et al. Nomogram for preoperative estimation of microvascular invasion risk in hepatitis B virus–related hepatocellular carcinoma within the Milan criteria. *JAMA surg*. 2016;151(4):356. doi:10.1001/jamasurg.2015.4257

35. Xu X, Zhang H-L, Liu Q-P, et al. Radiomic analysis of contrast-enhanced CT predicts microvascular invasion and outcome in hepatocellular carcinoma. *J Hepatol*. 2019;70(6):1133–1144. doi:10.1016/j.jhep.2019.02.023